J. Phys. B: At. Mol. Opt. Phys. **30** (1997) 2239–2259. Printed in the UK PII: S0953-4075(97)80664-5

Low-energy electron scattering from methane

C T Bundschu†, J C Gibson†, R J Gulley‡, M J Brunger§, S J Buckman†, N Sanna‖ and F A Gianturco¶

† Atomic and Molecular Physics Laboratories, Research School of Physical Sciences and Engineering, Australian National University, Canberra, ACT 0200, Australia
‡ CLRC Daresbury Laboratory, Daresbury, Warrington WA4 4AD, UK
§ Physics Department, Flinders University of South Australia, Bedford Park, SA 5042, Australia
‖ Supercomputing Centre for University and Research (CASPUR), Citta Universitaria, 00185, Rome, Italy
¶ Department of Chemistry, University of Rome, Citta Universitaria, 00185, Rome, Italy

Received 6 January 1997

Abstract. Absolute differential cross sections for elastic scattering and vibrational excitation ($\nu_{2,4}$, $\nu_{1,3}$) of CH_4 have been measured at incident energies between 0.6 and 5.4 eV. These cross sections have also been extrapolated and integrated in order to derive integral and momentum transfer cross sections which are compared with the results of previous single-collision and electron swarm experiments. Elastic differential cross sections have also been calculated using a body-fixed (BF), single-centre expansion (SCE) for the close-coupled (CC) equations. There is excellent agreement between the present data and the most recent elastic scattering results of Boesten and Tanaka, but substantial discrepancies between these two data sets and several previous measurements. There is also excellent agreement at most energies between the present measured and calculated elastic cross sections.

1. Introduction

Low-energy electron scattering from methane is of significant interest in many atmospheric and technological applications. CH_4 is an important constituent in the atmospheres of Jupiter, Saturn and our own planet, where it is one of the major greenhouse gases. An understanding of the complex chemistry of these atmospheres requires, amongst other things, a detailed knowledge of the cross sections for this gas in collision with low-energy electrons. Methane is also an active constituent in radiation detectors such as drift chambers and in diffuse discharge switches, where its deep Ramsauer–Townsend (RT) minimum, at around 0.35 eV, and resonantly enhanced scattering at higher energies (≈ 7.5 eV), results in a high conductivity gas for low-energy electrons. Furthermore, as it is the simplest organic molecule and essentially spherically symmetric, theoretical studies of electron–methane scattering have proved to be of considerable general interest in the development of electron–polyatomic molecule scattering theory.

As a result of the interest from these various areas, there has been a substantial number of measurements and calculations of scattering cross sections for methane in recent years. The most recent absolute elastic differential cross sections (DCS) for CH_4 are those of Boesten and Tanaka (1991) and Mapstone and Newell (1992). These measurements, both utilizing a crossed-beam geometry, were carried out at impact energies from 1.5–100 eV and 3–15 eV, respectively. Other elastic DCS for CH_4 have been measured by Sohn *et al* (1983, 1986)

0953-4075/97/092239+21$19.50

at energies between 0.1 and 5 eV, Tanaka *et al* (1982) (3–20 eV), Curry *et al* (1985) (7.5–20 eV) and Shyn and Cravens (1990) (5–50 eV). Müller *et al* (1985) have measured rotational excitation in both vibrationally elastic scattering and rovibrational excitation at energies of 0.5, 5, 7.5 and 10 eV. Near-threshold and resonant vibrational excitation cross sections have been studied by Rohr (1980), Sohn *et al* (1983), Tanaka *et al* (1983), Müller *et al* (1985), Curry *et al* (1985) and Shyn (1991). Excitation functions for total, elastic and inelastic cross sections below 6 eV and for vibrationally inelastic processes below 1.6 eV were studied by Lunt *et al* (1994). Absolute total cross sections were determined by Barbarito *et al* (1979), Ferch *et al* (1985), Jones (1985), Floeder *et al* (1985), Lohmann and Buckman (1986), Sueoka and Mori (1986), Dababneh *et al* (1988), Nishimura and Sakae (1990), Zecca *et al* (1991) and Kanik *et al* (1992).

There have been many calculations of low-energy elastic electron scattering from methane and, rather than document them all here, we shall only refer to relatively recent work in which references to the earlier work can be found. Bloor and Sherrod (1986) used the continuum multiple scattering approach to calculate total elastic cross sections for methane between 0–30 eV. Jain (1986a, b) used model potential approaches to calculate elastic and total scattering cross sections at low to intermediate energies while Yuan (1988) used spherical parameter-free model potentials for low-energy elastic scattering calculations. Lengsfield *et al* (1991) later applied the complex Kohn variational method to elastic scattering at low energies, Gianturco *et al* (1995a) calculated vibrationally elastic, rotationally summed cross sections for electron scattering from methane within the energy range from 0–10 eV and Althorpe *et al* (1995) have calculated integral elastic and vibrational excitation cross sections.

At energies below 3 eV the results of many of the above-mentioned measurements and theories are not in good agreement. The experimental results at times differ by almost a factor of two (e.g. the 1.5 eV elastic DCS measurements of Sohn *et al* and the more recent measurement by Boesten and Tanaka) and the present work was, in part, motivated by these discrepancies. The experimental apparatus and techniques are briefly summarized in the next section. Thereafter a summary of the present theoretical calculations is given, followed by the results and discussion section with some concluding remarks finally being drawn.

2. Apparatus and experimental techniques

The present measurements were carried out using a crossed-beam apparatus which has been described previously (Brunger *et al* 1990, Gulley *et al* 1994). Therefore we will only highlight the important features of its construction and operation here. The molecular beam is formed by quasi-effusive flow of methane through a multicapillary array. The electron beam is produced by a thoriated tungsten filament in conjunction with electrostatic electron optics and a hemispherical electron monochromator. This beam is crossed with the molecular beam and scattered electrons, either elastic or inelastic, are energy analysed and detected by a further combination of electron optics, hemispherical analyser and a channel electron multiplier. The overall energy resolution is typically 50 meV and the beam current in the interaction region ranged, depending on the beam energy, from 0.8–4 nA. The absolute incident energy was determined by calibrating the electron beam energy against the position of the second quasi-vibrational resonance peak in low-energy elastic scattering from N_2. At a scattering angle of 60° this peak occurs at an energy of 2.198 eV (Rohr 1977).

In order to place the angular distributions on an absolute scale, the relative flow technique has been employed (Khakoo and Trajmar 1986, Nickel *et al* 1989). The calculated elastic

helium cross sections of Nesbet (1979) are used as the reference standard for this process. The relative flow technique requires that the measurements for each gas (CH_4, He) are carried out under identical conditions. In the present experiments a number of measures have been taken towards achieving this goal: (i) both gases are always present in the scattering chamber; (ii) the driving pressures behind the capillary source are adjusted such that the gases have equivalent mean free paths in this region and (iii) the driving pressures are limited such that the mean free path of each gas is always greater than twice the diameter of the capillary tubes which form the array. These requirements on the driving pressures result in a gas pressure ratio of $p(CH_4)/p(\mathrm{He}) = 0.46$ and a maximum helium pressure of about 1.2 Torr. In order to be able to apply the relative flow technique the gas pressure, electron beam current and the scattered signal rates are measured at every angle and energy for both gases.

With the present energy resolution a study of vibrational excitation for the single modes (ν_1–ν_4) with excitation thresholds at 362, 190, 374 and 162 meV was not possible. However, the hybrid pairs $\nu_{2,4}$ (bending) and $\nu_{1,3}$ (stretching) are resolvable and the present inelastic cross section measurements are of these modes. The DCS measurements for these levels involved measuring an energy loss spectrum at each scattering angle. From these spectra the area under each of the energy loss features (elastic, $\nu_{2,4}$, $\nu_{1,3}$) was determined and the absolute DCS for each then determined from the relative flow measurements of the elastic scattering intensity in helium. The relative transmission of the analyser for elastic and inelastic electrons was optimized by scanning the zoom lenses in the analyser entrance optics in synchronization with the energy loss voltage. We estimate that this relative transmission does not vary by more than 10% for the range of incident and scattered energies covered here (Brunger *et al* 1991).

The absolute DCS for both elastic scattering and vibrational excitation were extrapolated and integrated to yield the corresponding integral cross sections (ICS). This was achieved, in the case of the elastic channel, by applying a version of an atomic phase-shift analysis routine to the (essentially) spherically symmetric CH_4 scattering system. Whilst the phase shifts derived from such a fit are of no particular physical significance it does provide a means, with some semi-quantitative physical basis, of extrapolating the DCS to forward and backward angles. For the vibrational excitation channels the extrapolation was done by eye. The derived integral cross sections have associated uncertainties of 12–15% (elastic) and 20–25% (vibrational) depending on the energy.

3. Computational details

The initial step of our computational treatment consists, as in our previous work (Gianturco *et al* 1995a, b), in the generation of the full, parameter-free, electron–molecule interaction potential given as local and non-local functionals of the electronic density of the target molecule. The latter was given in turn by its self-consistent-field (SCF), Hartree–Fock (HF) molecular orbitals (MOs) produced via a multicentre expansion over Gaussian-type analytic functions (GTOs).

We describe the collisional process in terms of the solution of the Schrödinger equation written in the form

$$\hat{H}\Psi(\boldsymbol{r}, \boldsymbol{x}) = E\Psi(\boldsymbol{r}, \boldsymbol{x}) \tag{1}$$

$$\hat{H}(\boldsymbol{r}, \boldsymbol{x}) = \hat{T}(\boldsymbol{r}) + \hat{V}(\boldsymbol{r}, \boldsymbol{x}) + H_{\mathrm{m}}(\boldsymbol{x}) \tag{2}$$

where $\hat{T}$ is the kinetic energy operator for the scattering electron, $\hat{V}$ is the electron–molecule interaction and H_{m} is the Hamiltonian of the molecular target. We let $\boldsymbol{x}$ represent collectively

the coordinates of the bound electrons and of the molecular nuclei and intend to refer all particles to a frame of reference fixed to the molecule (body-fixed (BF) frame).

The many-body problem in the scattering electronic coordinate $\boldsymbol{r}$ is now converted into an effective single-particle problem by expanding

$$\Psi(\boldsymbol{r}, \boldsymbol{x}) = \sum_{\alpha} A\{F_{\alpha}(\boldsymbol{r})\phi_{\alpha}(\boldsymbol{x})\} \tag{3}$$

where A is the antisymmetrization operator for the electronic coordinates, while the molecular nuclei are considered as being fixed in space during the scattering event (FN approximation).

By inserting equation (3) into (1) and multiplying the left-hand side by the conjugate of a representative state in the expansion (3), one obtains the familiar set of coupled integro-differential equations (IDEs)

$$\hat{H}_{\alpha} F_{\alpha}(\boldsymbol{r}) = \sum_{\beta} \xi_{\alpha\beta}(\boldsymbol{r}) \,. \tag{4}$$

In the above set of close-coupled (CC) equations for the scattering problem, the symbols are defined as

$$H_{\alpha} = \nabla_{\alpha}^2 + k_{\alpha}^2 \tag{5}$$

$$\xi_{\alpha\beta}(\boldsymbol{r}) = \int \hat{K}_{\alpha\beta}(\boldsymbol{r}, \boldsymbol{r}') F_{\beta}(\boldsymbol{r}') \, \mathrm{d}\boldsymbol{r}' \tag{6}$$

$$\hat{K}_{\alpha\beta}(\boldsymbol{r}, \boldsymbol{r}') = \hat{V}_{\alpha\beta}(\boldsymbol{r})\delta(\boldsymbol{r} - \boldsymbol{r}') + \hat{W}_{\alpha\beta}(\boldsymbol{r}, \boldsymbol{r}') \,. \tag{7}$$

Here k_{α}^2 is given by $2(E - \varepsilon_{\alpha})$, where E is the total collision energy and ε_{α} the molecular internal energy in the target state $|\alpha\rangle$. The local interaction involves, in our treatment, the exact electrostatic interaction with the target, $\hat{V}_{\mathrm{st}}$, and the linear response function of its electrons on the impinging projectile, the correlation–polarization potential $\hat{V}_{\mathrm{cp}}$. The latter was obtained using gradient-expansion corrections to a (DFT) treatment of short-range correlation (Gianturco *et al* 1993). The non-local interaction $\hat{W}_{\alpha\beta}$ describes the exchange potential between the bound and the continuum orbitals, obtained exactly via energy-optimized iterative schemes. In the case of only one single term in the expansion (3), the elastic scattering problem is then dealt with for a specific electronic state $|\alpha\rangle$ of the target molecule within the FN approximation (Gianturco *et al* 1994).

In order to solve the numerical problem as that of a set of coupled integro-differential radial equations, one now needs to expand both the bound $[\phi_i(x_i)]$, multicentre MOs and the continuum electron function $[F(\boldsymbol{r})]$ over a set of (SCE) symmetry-adapted angular partial waves X:

$$[\phi_i(\boldsymbol{x}_i)] = \sum_{h,l} r^{-1} u_{hl}^{i}(\boldsymbol{r}) X_{hl}^{p_i\mu_i}(\vartheta, \varphi) \tag{8a}$$

$$F_{p\mu}(\boldsymbol{r}) = \sum_{h,l} r^{-1} f_{hl}^{p\mu}(\boldsymbol{r}) X_{hl}^{p\mu}(\vartheta, \varphi) \,. \tag{8b}$$

Here $|i\rangle$ labels a specific, multicentre, occupied MO within the single-determinant description of the SCF-HF wavefunction of the target molecule. The indices of the continuum function and of each contribution $|p\mu\rangle$ label a relevant irreducible representation (IR) p and one of its components μ. The index h labels a specific basis, for the given partial wave l, used within the pth IR one is considering. The generalized, symmetry-adapted harmonics were given before and will not be discussed here again. The corresponding coefficients $u_{hl}^{i} = u_{hl}^{p_i\mu_i}$ are the essential ingredients for computing the interaction potentials

of (7) and were obtained here by numerical quadrature of the multicentre GTOs given as Cartesian Gaussian functions

$$g_\nu^{kj}(\boldsymbol{x}_k) = N(a,b,c;\alpha)x^a y^b z^c \exp(-\alpha \boldsymbol{x}_k^2) \tag{9a}$$

labelled by the kth atomic centre, of which g is the jth function, and by the contraction index ν of the primitive Gaussian within the subgroup that belongs to a given set of contraction coefficients d_ν,

$$G^{kj}(\boldsymbol{x}_k) = \sum_{\nu=1}^{\nu_{\max}} d_\nu^{kj} g_\nu^{kj}(\boldsymbol{x}_k)\,. \tag{9b}$$

The remaining parameters are included in the normalization constant N (see Gianturco *et al* 1995b) and the corresponding radial coefficients of (8*a*) are thus given by the angular quadratures over the corresponding polar coordinates (Gianturco *et al* 1994).

The quadratures were carried out via a Gauss–Laguerre procedure using a discrete, variable radial grid, for each point of which the spherical grid in the (ϑ, ϕ) points was evaluated. Convergence was achieved with grids of 46×46 sets of angular points, while up to 500 radial values were generated in the centre of mass of the molecular target (BF frame). Several numerical tests were carried out using different grids and the final results can be considered converged (on the wavefunction representation) to within less than 1%. A further discussion of the accelerated convergence for the iterative exchange approach was already given in our previous work (Gianturco *et al* 1994).

The SCE implementation was carried out, in a symmetry-adapted form, for all the potential contributions of (7) and for both the bound and the continuum orbitals of (8), up to $l_{\max} = 10$. The IR considered in the calculations were the A_1, the T_2, and the E symmetries for the continuum orbitals, while only the a_1 and the t_2 symmetries are occupied in the $^1A_1$ ground electronic state of the target molecule.

Convergence tests on the partial-wave expansion were carried out in all the symmetries. In our previous work on this system (Gianturco *et al* 1995a, b) we could clearly see that all cross sections have essentially converged with $l_{\max} = 7$, which means five coupled IDEs for the scattering process in the A_1 symmetry.

It is also interesting to note that, when using an approximate form for $\hat{W}_{\alpha\beta}$ in equation (7), it is usually suggested that the continuum functions should be forced to be orthogonal to the bound orbitals of the same symmetry in order to guarantee the right nodal structure of all $N + 1$ orbitals within the physical space of the molecular charge density.

The present results were obtained instead using the exact exchange interaction, whereby the final scattering orbitals at the (SE) levels are correctly obtained to be orthogonal to the bound orbitals of the same symmetry, as required theoretically. The corresponding K-matrix elements of the above BF-FN calculations were in turn transformed to the space-fixed (SF) frame of reference and employed to obtain the angular distributions at the energies for which the experimental data have been collected. The detailed comparisons with the present measurements, with earlier measurements, and with other theoretical calculations are shown in the following section.

4. Results and discussion

4.1. Elastic scattering

The absolute elastic differential cross sections for CH_4, at eight incident energies between 0.6 and 5.4 eV, are presented in table 1. Examples of these cross sections are shown in figures 1–6 where they are also compared with previous experimental results and recent theoretical calculations.

Table 1. Absolute elastic differential cross sections (in units of 10^{-16} cm^2 sr^{-1}) for electron scattering from methane. The figures in parentheses represent the absolute uncertainty expressed as a percentage. Integral cross sections at the foot of each column are in units of 10^{-16} cm^2.

	Energy (eV)							
Angle	0.6	1.0	1.5	1.7	2.0	3.0	5.0	5.4
12							3.913(8.0)	4.875(7.5)
15						0.556(10)	3.386(6.6)	4.238(6.6)
17.5					0.177(19)			
20			0.085(35)	0.103(21)		0.380(6.5)	2.601(6.4)	3.344(6.6)
22.5					0.124(16)			
25				0.057(20)		0.354(6.6)	2.046(7.1)	2.580(6.4)
27.5					0.122(16)			
30		0.020(31)	0.043(25)	0.052(12)		0.356(7.2)	1.643(6.8)	2.049(6.4)
32.5					0.154(8.5)			
35	0.068(47)			0.066(12)		0.441(6.9)	1.364(6.7)	1.689(6.4)
40	0.040(44)	0.026(41)	0.104(9.2)	0.128(7.3)		0.558(7.4)	1.261(6.4)	1.501(6.4)
42.5					0.321(7.1)			
45							1.283(7.2)	1.416(6.4)
50	0.035(30)	0.081(14)	0.234(7.7)	0.274(8.4)		0.845(6.4)	1.328(7.4)	1.446(6.6)
52.5					0.551(6.5)			
55							1.474(6.5)	1.528(6.4)
60	0.038(45)	0.158(14)	0.374(7.0)	0.444(6.9)		1.123(7.3)	1.589(6.5)	1.627(6.3)
62.5					0.752(6.4)			
65				0.519(6.5)		1.236(7.1)	1.710(6.4)	1.716(6.4)
67.5					0.820(6.6)			
70	0.040(23)	0.227(13)	0.475(7.2)	0.557(7.1)		1.298(6.5)	1.819(6.6)	1.806(6.4)
72.5					0.850(6.5)			
75				0.592(6.7)		1.32(7.6)	1.829(6.3)	1.807(6.3)
77.5					0.850(6.8)			
80	0.068(18)	0.275(7.8)	0.524(6.8)	0.611(6.7)		1.25(6.8)	1.786(6.4)	1.751(6.3)
82.5					0.847(6.8)			
85				0.615(7.0)			1.636(6.5)	1.618(6.3)
87.5					0.806(6.8)			
90	0.100(20)	0.272(8.4)	0.484(6.9)	0.588(6.5)		1.028(6.8)	1.471(6.5)	1.437(6.4)
92.5					0.705(6.6)			
95							1.194(6.7)	1.172(6.5)
100	0.112(16)	0.263(8.8)	0.424(6.7)	0.490(6.5)		0.758(6.5)	0.962(6.5)	0.935(6.4)
102.5					0.569(12)			
105							0.681(7.6)	0.658(6.4)
110	0.100(12)	0.221(9.8)	0.329(6.7)	0.375(6.8)		0.431(6.6)	0.452(7.3)	0.427(6.8)
112.5					0.343(7.1)			
115							0.266(8.0)	0.246(6.4)
120	0.127(27)	0.180(11)	0.216(7.8)	0.241(6.5)		0.194(11.4)	0.160(8.5)	0.153(6.4)
122.5					0.178(7.4)			
125						0.111(9.8)	0.148(6.6)	0.161(6.4)
130	0.128(41)	0.131(12)	0.138(20)	0.140(10)		0.109(8.2)	0.236(6.8)	0.280(6.4)
132.5					0.084(10)			
σ_i	1.10	1.78	3.58	4.38	5.73	9.13	17.49	18.96
σ_M	1.06	2.02	3.23	3.79	4.64	7.70	15.92	17.25

At 0.6 eV (figure 1) we compare the present results with those of Sohn *et al* (1986). Whilst the agreement in shape between these two data sets is reasonably good, there are substantial differences in their magnitudes, although we note that the uncertainty on the

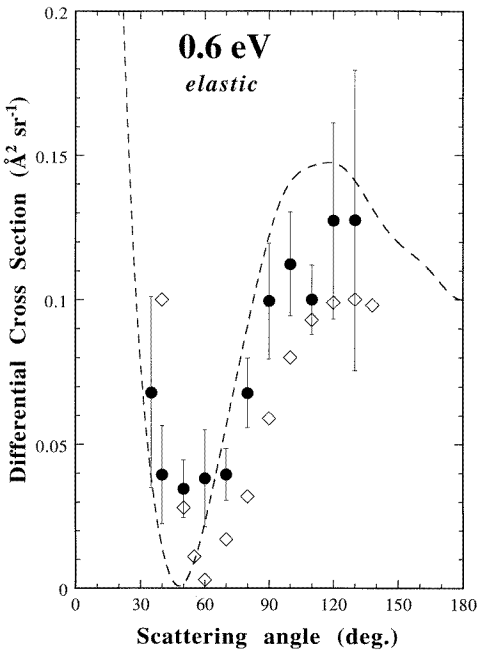

Figure 1. Absolute differential cross sections for elastic electron scattering from methane at 0.6 eV. ●, present results; ◇, Sohn *et al* (1986); – – –, present calculation.

present data set is considerable at this energy and the cross sections are extremely small. Nonetheless this observation is consistent with previous comparisons between data from these two laboratories for other systems, such as CO and N_2, where there are similar differences in magnitude. Comparison can also be made against the present theoretical calculation with the level of agreement being remarkably good, given the large experimental uncertainties. The distinct minimum found in the experiments at about 60° is reproduced in the theory as is the maximum at about 120°.

At an energy of 1 eV, for reasons of clarity, we present the comparison in two figures (figures 2(*a*) and (*b*)). In figure 2(*a*) the present data are once again considerably higher ($\approx 20\%$) than those of both Rohr (1980) and Sohn *et al*, which match each other quite well, particularly near the cross section maximum at around 90°. However, the data of Rohr and Sohn *et al* are in better agreement with the present measurements at the more extreme forward and backward angles. There are several theoretical cross sections available at this energy for comparison with experiment. The present calculation is compared with the present and previous experiments in figure 2(*a*) and the present data are compared with the previous calculations in figure 2(*b*). Whilst most of the calculations show the same general shape as that of the experimental values, the empirical results of Bloor and Sherrod (1986) exhibit what seems to be the closest agreement with the present measurements over a broad range of angles. The present calculations, which do not have any adjustable parameter in their treatment of the interaction, also follow the experiments very closely, although they indicate a larger maximum in the DCS around 80° than that found in the present measurements. The other calculations (Jain 1986a, b, McNaughten *et al* 1990) are lower than both the present measurements and calculations at most angles, but, although it is not shown explicitly in figure 2(*b*), the former of these is in better agreement with the DCS of Sohn *et al*.

The results shown in figure 3 for an incident energy of 1.5 eV, indicate that the measurements of Boesten and Tanaka (1991) are in very good agreement with the present

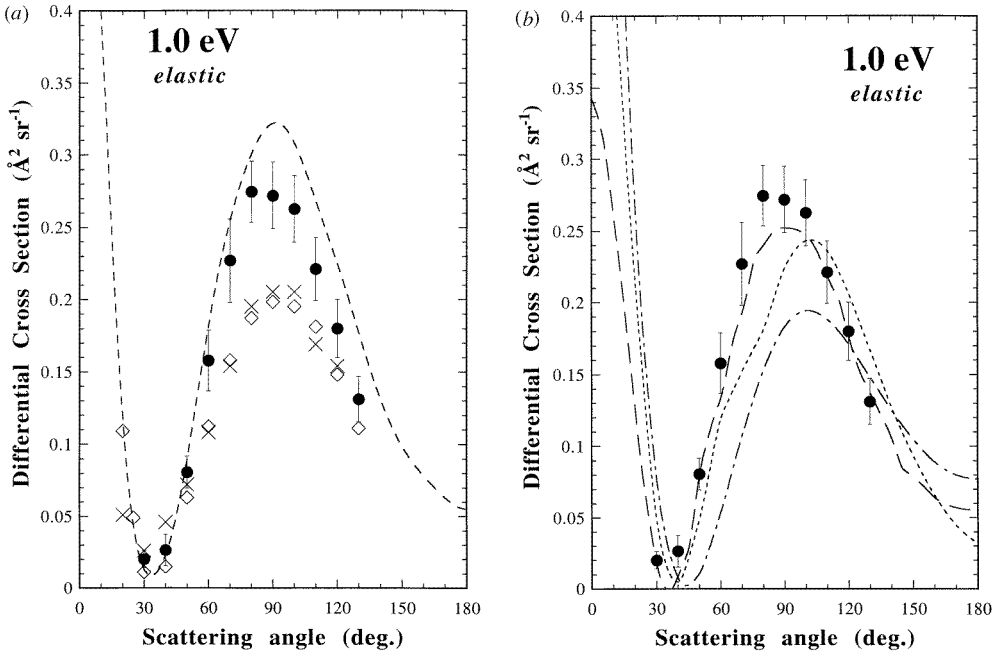

Figure 2. Absolute differential cross sections for elastic electron scattering from methane at 1.0 eV. (*a*) ●, present results; ×, Rohr (1980); ◇, Sohn *et al* (1986); – – –, present calculation. (*b*) ●, present results; — — —, Bloor and Sherrod (1986); — · —, Jain (1986a, b); - - -, McNaughten *et al* (1990).

data, with the data points overlapping at almost all scattering angles when the combined experimental uncertainties are taken into account. The data of Sohn *et al* (1986) are once again in good agreement with regard to the shape of the cross section, but consistently smaller in magnitude (≈ 20%), than the present measurements at angles larger than 30°. At this energy the present calculations yield a cross section that is higher than the present experiment at most angles by 10–20%, although the level of agreement with regard to the general shape is excellent. At this collision energy we also show the DCS resulting from the phase-shift analysis of the experimental data. This indicates that such an approach can indeed provide a reasonable method for the extrapolation of the experimental DCS to the inaccessible angular regions to aid the calculation of integral cross sections.

At 2 eV (figure 4) there is once again reasonably good agreement between the present data and those of Boesten and Tanaka although the present cross section is consistently larger, with the differences in magnitude, at times, lying outside the combined experimental uncertainties of the two data sets (≈15–20%). The cross section of Rohr is again consistently lower in magnitude (20–30%) than both the present cross section and that of Boesten and Tanaka. Qualitatively speaking there is good agreement in shape between all the measurements: they all show a maximum at about 90° and a minimum at about 30°. The present calculations and the empirical results of Bloor and Sherrod are very similar in shape and magnitude and both are in excellent agreement with the present measurement across the whole angular range.

In figure 5 we provide a comparison of the results of the present measurements at 3.0 eV with the experiments of Rohr (1980), Sohn *et al* (1986), Boesten and Tanaka (1991) and

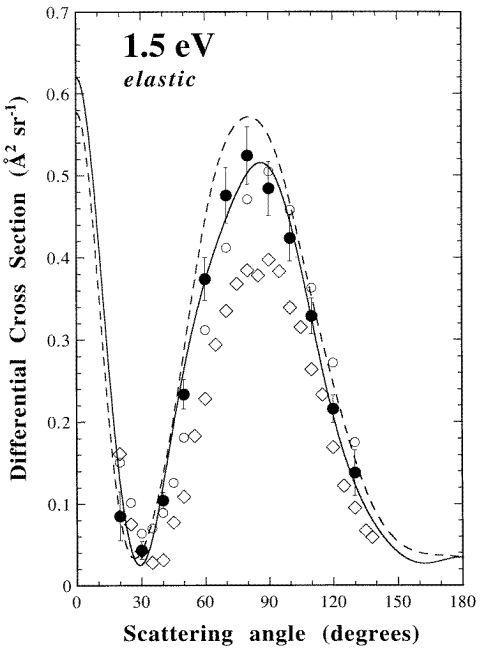

Figure 3. Absolute differential cross sections for elastic electron scattering from methane at 1.5 eV. ●, present results; ◇, Sohn *et al* (1986); ○, Boesten and Tanaka (1991); – – –, present calculation; —— phase-shift analysis of present DCS data.

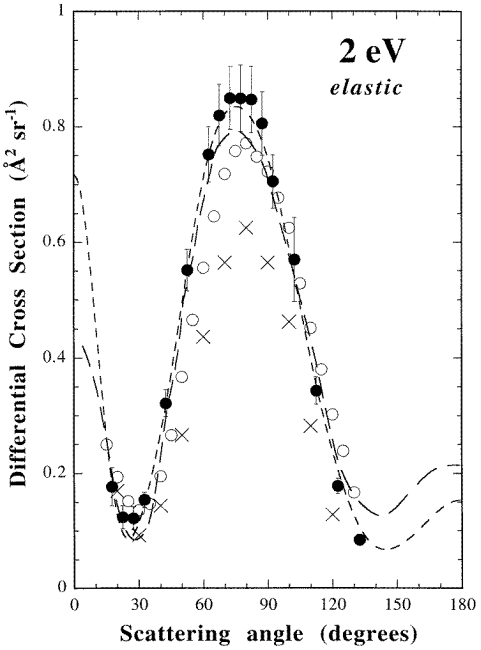

Figure 4. Absolute differential cross sections for elastic electron scattering from methane at 2 eV. ●, present results; ×, Rohr (1980); ○, Boesten and Tanaka (1991); – – –, present calculation; — — —, Bloor and Sherrod (1986).

Mapstone and Newell (1992), the latter cross section having being measured at 3.2 eV. Once again, for reasons of clarity, the comparison between the various experiments and the present calculation is made in figure 5(*a*) whilst that between the present experiment and previous theory is given in figure 5(*b*). The agreement between the present measurements and those of Boesten and Tanaka is excellent over the whole angular range. The DCS of Sohn *et al* predicts the position and the magnitude of the two minima very well, but they once again appear to underestimate the absolute magnitude of the cross section in the mid-angular region. The results of Mapstone and Newell are in poor agreement with the present measurements particularly in the region of the mid-angle, cross section peak where they are about 40% smaller than the present results. On the other hand their DCS are slightly larger in magnitude than the present ones at both forward and backward angles. In figure 5(*b*) the semiempirical calculations of McNaughten *et al* (1990) describe the behaviour of the cross section at higher angles ($> 70^\circ$) extremely well, whilst at forward angles there are discrepancies in both the magnitude and shape of the cross section. The calculation of Jain and Thompson (1982) is in quite good qualitative agreement with the present DCS but it overestimates the magnitude at angles between 20–70°. The theory of Lengsfield *et al* describes the cross section in the region of the second minimum very well, but it fails to predict the magnitude of the maximum and the rising cross section at angles below 30°. On the other hand, the present calculated DCS is in excellent agreement with the present measured DCS at all scattering angles.

At 5 eV (figure 6) the present data and those of Boesten and Tanaka are again in excellent agreement, with the exception of very forward angles ($< 20^\circ$) where the present

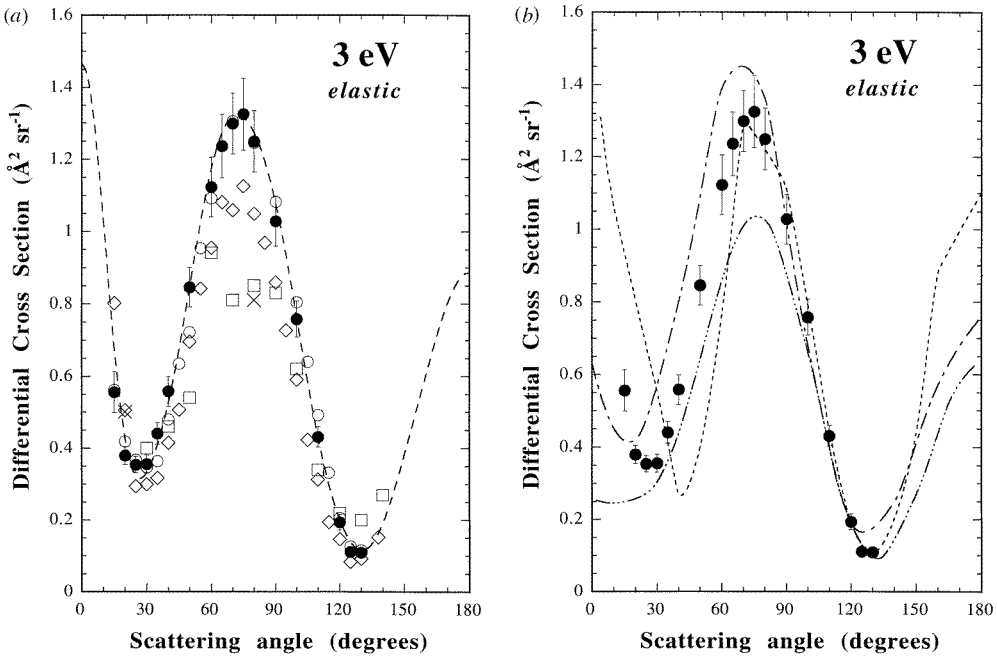

Figure 5. Absolute differential cross sections for elastic electron scattering from methane at 3 eV. (*a*) ●, present results; ×, Rohr (1980); ◇, Sohn *et al* (1986); ○, Boesten and Tanaka (1991); □, Mapstone and Newell (1992) at 3.2 eV; — — —, present calculation. (*b*) ●, present results; — · —, Jain and Thompson (1982); – – –, McNaughten *et al* (1990); — · · · —, Lengsfield *et al* (1991).

DCS is ≈20% higher. The other experimental cross sections (Sohn *et al* 1986, Rohr 1980) are in very good agreement with the present DCS in the region of the second minimum, but they both underestimate the cross section at scattering angles between 40° and 100°. The present calculations are in very good agreement with the present measurements, while the theoretical cross sections of both Jain and McNaughten *et al*, although they predict the position and magnitude of the second minima very well, fail to correctly predict the first two extrema. On the other hand, the empirical calculations of Bloor and Sherrod are in very good accord with the present measurements, although the extent to which they can be used in a quantitative comparison with the experiment is hard to judge, given the number of arbitrary parameters that are used in their calculation.

4.2. Vibrationally inelastic scattering

Absolute DCS for vibrational excitation ($\nu_{2,4}$, $\nu_{1,3}$) of methane at energies between 1.0 and 5.0 eV are given in tables 2 and 3. A comparison of the present results with other experimental data is given in figures 7–10. As was mentioned previously, in the present measurements we were not able to resolve the single vibrational modes (ν_1, ν_2, ν_3, ν_4) while it was possible to resolve the hybrid $\nu_{2,4}$ (bending) and $\nu_{1,3}$ (stretching) modes. At the lower energies, signal levels were extremely low and in some cases large statistical errors are evident on the individual data points. We have measured the $\nu_{2,4}$ differential cross section at 1, 2, 3 and 5 eV and the $\nu_{1,3}$ cross section at 2, 3 and 5 eV. In order to obtain integral cross sections we have also graphically extrapolated the measured DCS to 0° and to 180° before integrating them to yield the corresponding integral cross sections.

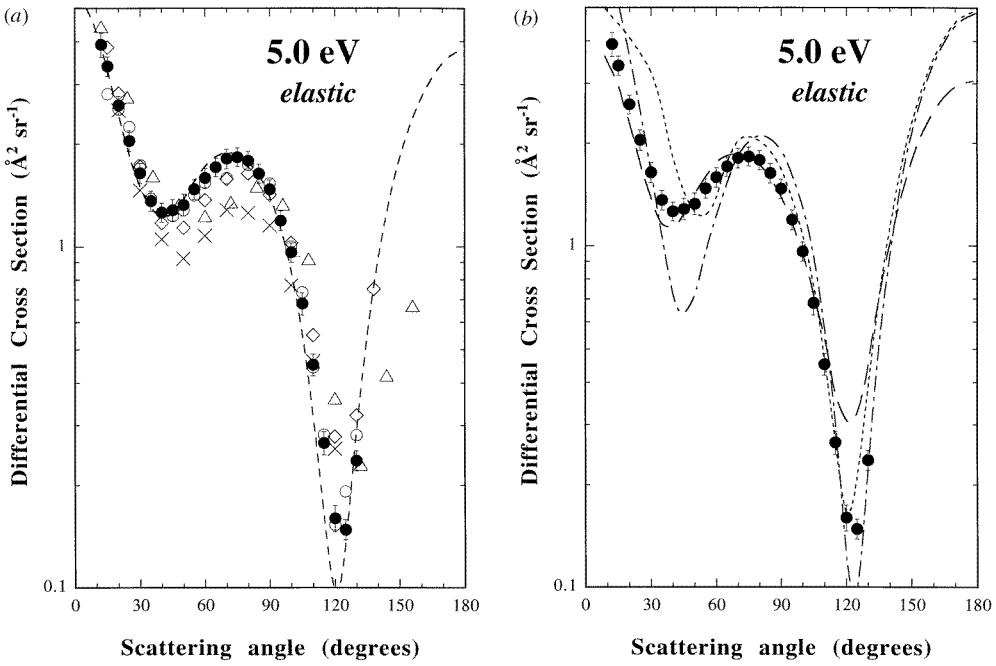

Figure 6. Absolute differential cross sections for elastic electron scattering from methane at 5 eV. (*a*) ●, present results; ×, Rohr (1980); ◇, Sohn *et al* (1986); ○, Boesten and Tanaka (1991); △, Shyn and Cravens (1990); – – –, present calculation. (*b*) ●, present results; — · —, Jain (1986a, b); - - - -, McNaughten *et al* (1990); – – –, Bloor and Sherrod (1986).

The measured DCS for the two composite modes show similar angular distributions and absolute magnitudes at each energy, although in most cases the stretching modes show a slightly stronger scattering at forward angles. As each composite is made up of one Raman active mode (ν_3 and ν_4) and as all modes are infrared active, it is unfortunately not possible to be specific about the relative contributions from these modes to each cross section. This aspect has been addressed, however, by Müller *et al* (1985). At 1 eV the present $\nu_{2,4}$ vibrational excitation cross section is compared with that of Sohn *et al*, in figure 7, with the latter being consistently smaller in magnitude than the present results by 30–40%. Given that their elastic DCS were also smaller than the present elastic data, and each cross section has been measured relative to the elastic scattering strength, this is perhaps not surprising. Both cross sections show essentially isotropic scattering between 60° and 130°.

At 2 eV (figure 8) our $\nu_{2,4}$ and $\nu_{1,3}$ cross sections are compared with the only other available experimental data, those of Rohr (1980). Once again the present $\nu_{2,4}$ cross section (figure 8(*a*)) is consistently higher than that of Rohr, in this case by about a factor of 2, although qualitatively there is good agreement in the shape of the two DCS. The present $\nu_{1,3}$ cross section (figure 8(*b*)), on the other hand, agrees quite well in both magnitude and shape with that of Rohr. This observation is somewhat puzzling and can only be indicative of some significant difference in the relative transmission of the two spectrometers.

A similar situation also exists at an energy of 3 eV. In this case, however, we can further compare our results with the experimental data of Tanaka *et al* (1983). Here the present data are considerably larger (by about a factor of 3) than the cross section of Tanaka *et al*

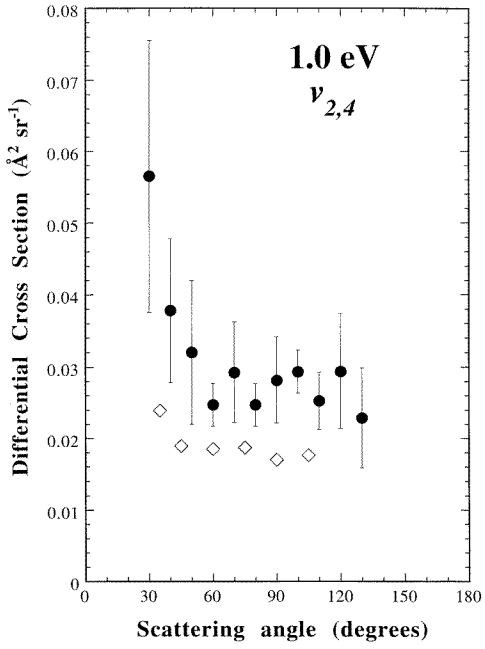

Figure 7. Absolute differential cross sections for excitation of the $\nu_{2,4}$ composite vibrational mode of methane at an incident energy of 1 eV. ●, present results; ◇, Sohn *et al* (1986).

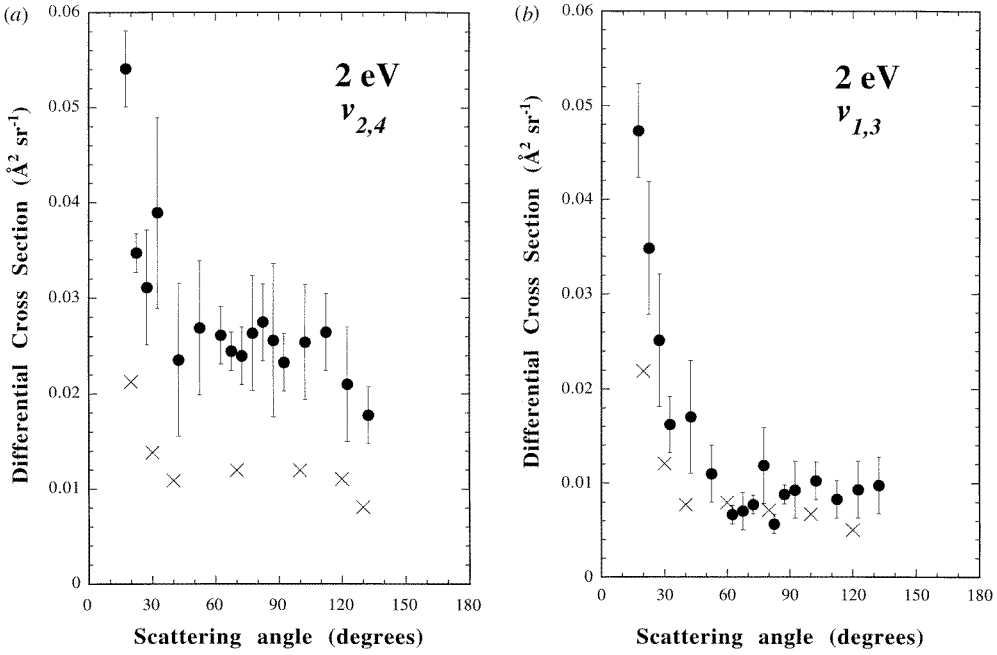

Figure 8. Absolute differential cross sections for excitation of the (*a*) $\nu_{2,4}$ and (*b*) $\nu_{1,3}$ composite vibrational modes of methane at an incident energy of 2 eV. ●, present results; ×, Rohr (1980).

and the lone point of Rohr (obtained from his published excitation functions) for the $\nu_{2,4}$ excitation (figure 9(*a*)). On the other hand, for the $\nu_{1,3}$ cross section (figure 9(*b*)) the agreement in magnitude, whilst by no means perfect, is substantially better. Both of the

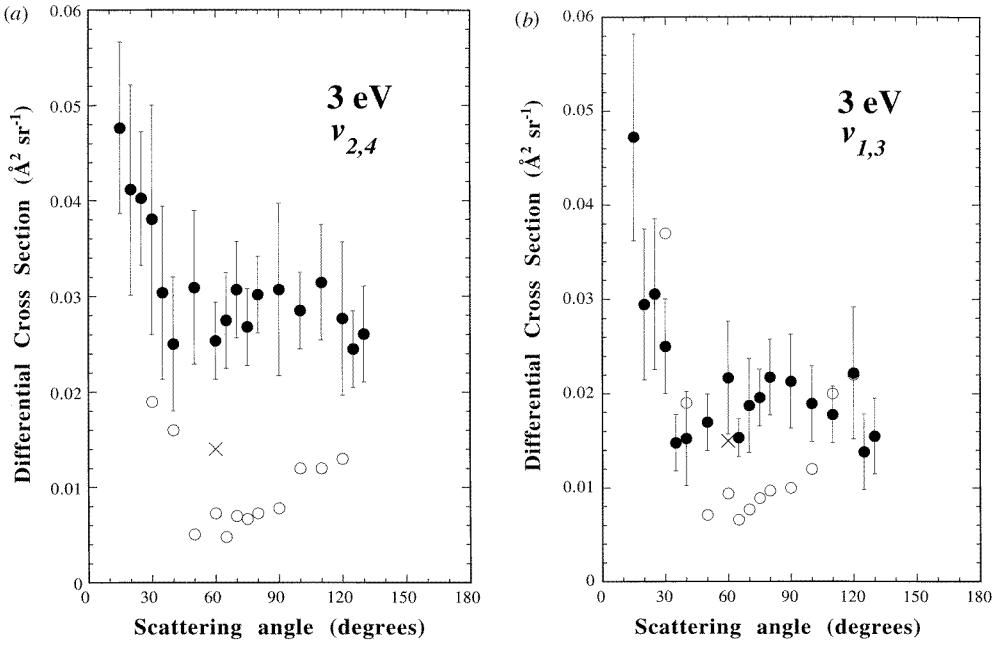

Figure 9. Absolute differential cross sections for excitation of the (*a*) $\nu_{2,4}$ and (*b*) $\nu_{1,3}$ composite vibrational modes of methane at an incident energy of 3 eV. ●, present results; ×, Rohr (1980); ○, Tanaka *et al* (1983).

present $\nu_{1,3}$ and $\nu_{2,4}$ DCS also show the hint of an emerging d-wave angular dependence, which is not present in the cross section of Tanaka *et al*, but which is consistent with the increasingly resonant nature of the scattering, even at 3 eV (see, e.g., Rohr 1980).

At 5 eV (figure 10) the overall situation is even further confused when the present DCS is compared with the measurements of Tanaka *et al* and the relatively recent cross sections of Shyn (1991). Once again the present $\nu_{2,4}$ cross section (figure 10(*a*)) is substantially larger, again by about a factor of two, at all but the most forward angles when compared to the measurements of both Tanaka *et al* and Shyn. Despite this difference there is reasonable qualitative accord between all these measurements regarding the shape of the DCS, including the weak indication of a d-wave behaviour. For the $\nu_{1,3}$ excitation (figure 10(*b*)), the present cross section is in good agreement, both in shape and magnitude, with the measurement of Shyn and both of them indicate the presence of strong, resonant d-wave contributions. On the other hand they both disagree substantially with the cross section of Tanaka *et al* (1982).

4.3. Integral cross sections for elastic scattering and vibrational excitation

The present DCS for elastic and inelastic scattering have been extrapolated to forward and backward angles and integrated in order to calculate integral elastic, elastic momentum transfer, integral vibrationally inelastic (for the $\nu_{2,4}$ and $\nu_{1,3}$ composite modes) and grand total cross sections. In the case of elastic scattering the extrapolation was facilitated by the previously discussed phase-shift analysis whilst, for the vibrational DCS, it was done by graphical means. The integral elastic and inelastic cross sections have also been combined, where possible, to yield the grand total cross section. These integral cross sections are given

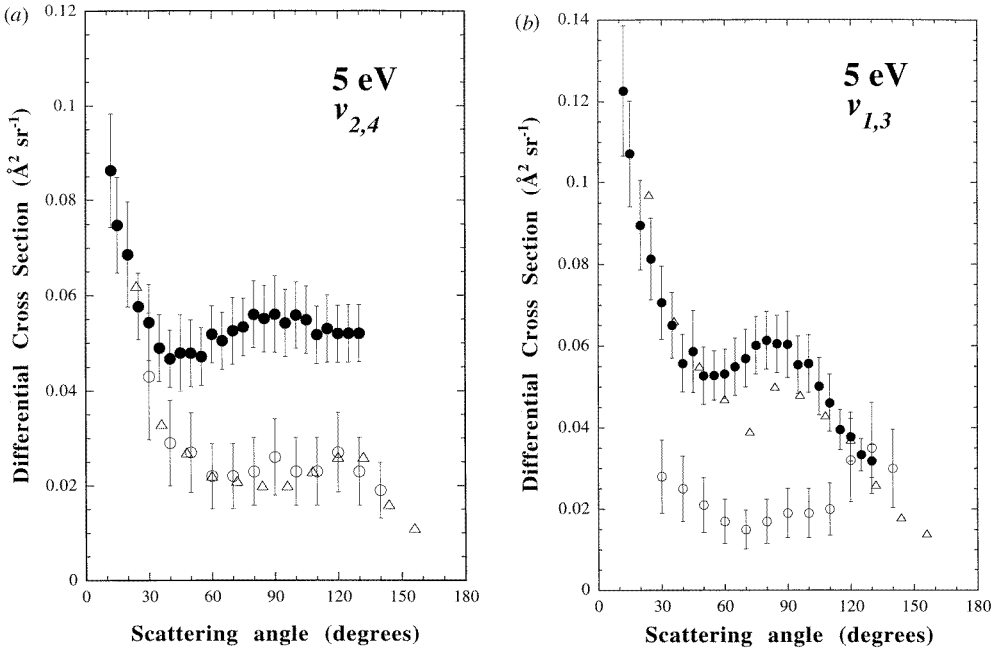

Figure 10. Absolute differential cross sections for excitation of the (*a*) $\nu_{2,4}$ and (*b*) $\nu_{1,3}$ composite vibrational modes of methane at an incident energy of 5 eV. ●, present results; ○, Tanaka *et al* (1982); △, Shyn (1991).

at the base of each of the differential cross section tables and the grand total cross section represents their sum whenever applicable.

The data for the integral elastic cross section are compared in figure 11 to the corresponding cross sections derived by Sohn *et al* and Boesten and Tanaka, both of which were obtained from a phase-shift analysis of their DCS data. The most recent calculations of Althorpe *et al* are also shown in the figure. As may be expected, following the comparison already made at the differential level, the integral cross section of Sohn *et al* is slightly smaller in magnitude than the present one, although they clearly overlap within the associated uncertainties ($\approx 20\%$), whilst that of Boesten and Tanaka is in excellent agreement with the present experiment. With the exception of the lower energy points at 0.6 and 1.0 eV, there is also very good agreement between the present measurement and the calculation of Althorpe *et al*.

For the grand total cross section (figure 12) we compare the present experimental results with the time-of-flight attenuation data of Ferch *et al* (1985) and Lohmann and Buckman (1986), the differential-derived data of Sohn *et al* (1986) and the attenuation measurements of Zecca *et al* (1991) and Kanik *et al* (1992). Note that the contribution from vibrational excitation in the region of the Ramsauer–Townsend minimum is significant and, as a result, we have not included the present measurement at 0.6 eV where we only have elastic DCS data. The level of agreement between the various results at energies of 1 eV and above is excellent.

In figure 13 we show the present elastic momentum transfer cross section and compare it with the crossed-beam measurements of Sohn *et al* and Boesten and Tanaka, and also with the swarm-derived cross sections of Haddad (1985), Schmidt (1991) and Hildebrandt

Table 2. Absolute differential cross sections for excitation of the composite $\nu_{2,4}$ vibrational modes of methane in units of 10^{-16} cm^2 sr^{-1}. The figures in parentheses represent the absolute uncertainty expressed as a percentage. Integral cross sections are given in units of 10^{-16} cm^2.

	Energy (eV)				
Angle	1	2	3	5	5.4
12				0.086(14)	0.090(13)
15			0.048(19)	0.075(13)	0.078(12)
17.5		0.054(7.7)			
20			0.041(27)	0.069(16)	0.069(13)
22.5		0.035(7.2)			
25			0.040(18)	0.058(12)	0.062(12)
27.5		0.031(18)			
30	0.057(34)		0.038(32)	0.054(14)	0.057(12)
32.5		0.039(25)			
35			0.030(28)	0.049(14)	0.053(12)
40	0.037(26)		0.025(29)	0.047(13)	0.051(12)
42.5		0.024(34)			
45				0.048(17)	0.049(12)
50	0.032(31)		0.031(27)	0.048(14)	0.053(17)
52.5		0.027(26)			
55				0.047(12)	0.051(15)
60	0.025(12)		0.025(14)	0.052(12)	0.049(12)
62.5		0.026(11)			
65			0.027(18)	0.050(12)	0.050(12)
67.5		0.024(7.6)			
70	0.029(23)		0.031(16)	0.053(12)	0.052(12)
72.5		0.024(13)			
75			0.027(16)	0.053(12)	0.052(12)
77.5		0.026(21)			
80	0.025(13)		0.030(14)	0.056(12)	0.054(12)
82.5		0.027(15)			
85				0.055(12)	0.055(12)
87.5		0.026(30)			
90	0.028(21)		0.031(28)	0.056(13)	0.055(12)
92.5		0.023(12)			
95				0.054(12)	0.056(12)
100	0.029(12)		0.028(13)	0.056(12)	0.057(12)
102.5		0.025(24)			
105				0.055(12)	0.055(12)
110	0.025(15)		0.031(20)	0.052(12)	0.055(12)
112.5		0.026(14)			
115				0.053(12)	0.055(12)
120	0.029(28)		0.028(27)	0.052(12)	0.054(12)
122.5		0.021(27)			
125			0.024(15)	0.052(12)	0.054(12)
130	0.023(29)		0.026(18)	0.052(12)	0.055(12)
132.5		0.018(16)			
σ_i	0.384	0.206	0.245	0.673	0.700

(1996). In the energy region of the present measurements, 0.6–5.4 eV, the level of agreement between all of these cross sections is reasonably good. There are substantial discrepancies between the various swarm measurements and the beam-derived measurement of Sohn *et al* in the region of the R–T minimum and, whilst the present measurements do not extend to

Table 3. Absolute differential cross sections for excitation of the composite $\nu_{1,3}$ vibrational modes of methane in units of 10^{-16} cm^2 sr^{-1}. The figures in parentheses represent the absolute uncertainty expressed as a percentage. Integral cross sections are in units of 10^{-16} cm^2.

	Energy (eV)			
Angle	2	3	5	5.4
12			0.123(13)	0.129(12)
15		0.047(23)	0.107(12)	0.118(12)
17.5	0.047(11)			
20		0.029(27)	0.090(13)	0.102(12)
22.5	0.035(21)			
25		0.031(25)	0.081(12)	0.089(12)
27.5	0.025(27)			
30		0.025(21)	0.071(12)	0.079(12)
32.5	0.016(21)			
35		0.015(18)	0.065(12)	0.071(12)
40		0.015(32)	0.056(12)	0.064(12)
42.5	0.017(33)			
45			0.059(16)	0.060(12)
50		0.017(20)	0.053(13)	0.061(15)
52.5	0.011(28)			
55			0.053(12)	0.059(17)
60		0.022(26)	0.053(12)	0.057(12)
62.5	0.0067(17)			
65		0.015(14)	0.055(12)	0.058(12)
67.5	0.0070(23)			
70		0.019(28)	0.057(13)	0.061(12)
72.5	0.0077(17)			
75		0.020(14)	0.060(12)	0.062(12)
77.5	0.0119(36)			
80		0.022(20)	0.061(12)	0.063(12)
82.5	0.0057(26)			
85			0.060(12)	0.063(12)
87.5	0.0088(14)			
90		0.021(25)	0.060(13)	0.063(12)
92.5	0.0093(31)			
95			0.055(12)	0.060(12)
100		0.019(19)	0.056(12)	0.058(12)
102.5	0.0103(24)			
105			0.050(14)	0.052(12)
110		0.018(14)	0.047(16)	0.048(12)
112.5	0.0083(24)			
115			0.040(13)	0.044(12)
120		0.022(33)	0.038(17)	0.039(12)
122.5	0.0093(30)			
125		0.014(31)	0.033(12)	0.037(12)
130		0.015(26)	0.033(13)	0.035(12)
132.5	0.0098(30)			
σ_i	0.079	0.204	0.651	0.689

low enough energies to clearly resolve this issue, it is possible to draw some conclusions from the trends in the present data. Firstly, at 0.6 eV, where there is about an order of magnitude difference between the cross section of Haddad and that of Hildebrandt, the present measurements clearly favour the former. Secondly, given that the present DCS

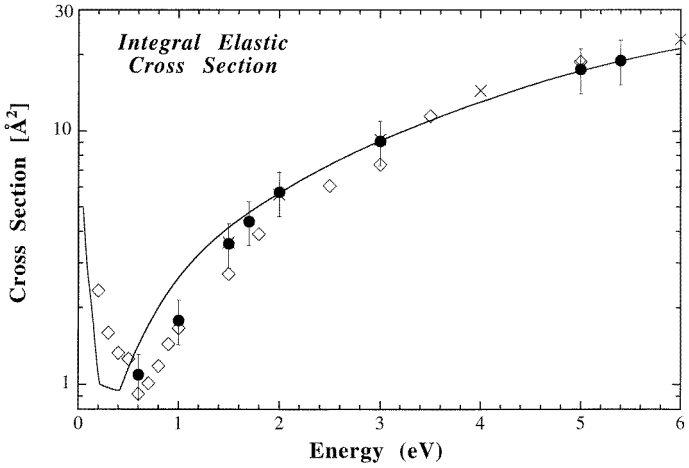

Figure 11. Integral elastic cross section for methane from 0–6 eV. ●, present results; ◇, Sohn *et al* (1986); ×, Boesten and Tanaka (1991); ——, Althorpe *et al* (1995).

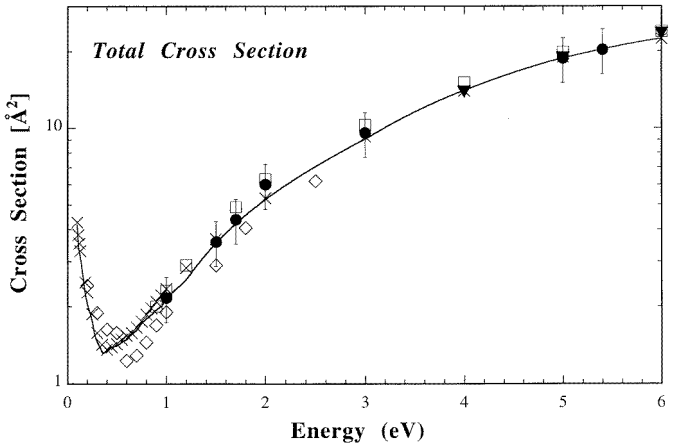

Figure 12. Grand total cross section for electron scattering from methane between 0 and 6 eV. ●, present results; ×, Ferch *et al* (1985); ——, Lohmann and Buckman (1986); ◇, Sohn *et al* (1986); □, Zecca *et al* (1991); ▼, Kanik *et al* (1992).

measurements display good qualitative (shape) agreement with those of Sohn *et al* at all energies, but are typically 20–30% larger in absolute magnitude, we would conclude that the beam-derived measurements, in general, favour the larger cross section of Haddad in the R–T minimum region.

Figure 14 compares the present total vibrational cross section for the composite $\nu_{2,4}$ mode with those of Shyn (1991), Tanaka *et al* (1983) and cross sections derived from swarm experiments by Haddad (1985), Schmidt (1991), and Hildebrandt (1996). The overall agreement at energies below 3 eV is reasonably good, and the present experiments show particularly good agreement with the calculation of Althorpe *et al* (1995), over the fairly broad energy range from 1–6 eV, and with the measured cross section of Hildebrandt at 1 and 2 eV. The nature of the low-energy structure in the latter cross section is not at all clear. Whilst several experiments have indicated near-threshold structure in the

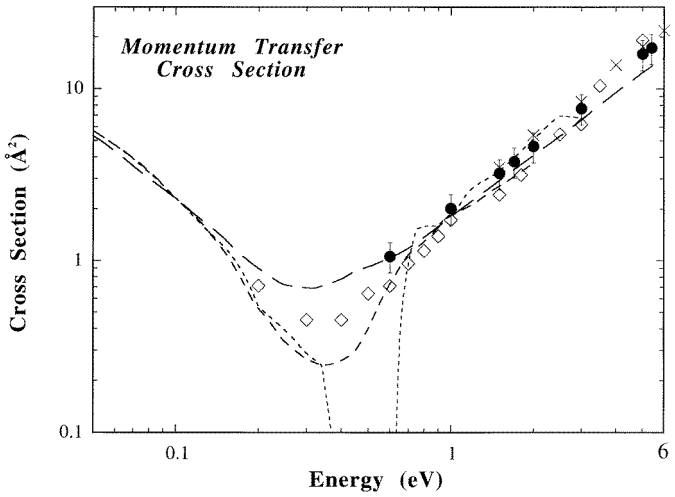

Figure 13. Elastic momentum transfer cross section for methane between 0 and 6 eV. ●, present results; ◇, Sohn *et al* (1986); ×, Boesten and Tanaka (1991); — — —, Haddad (1985); – – –, Schmidt (1991); - - -, Hildebrandt (1996).

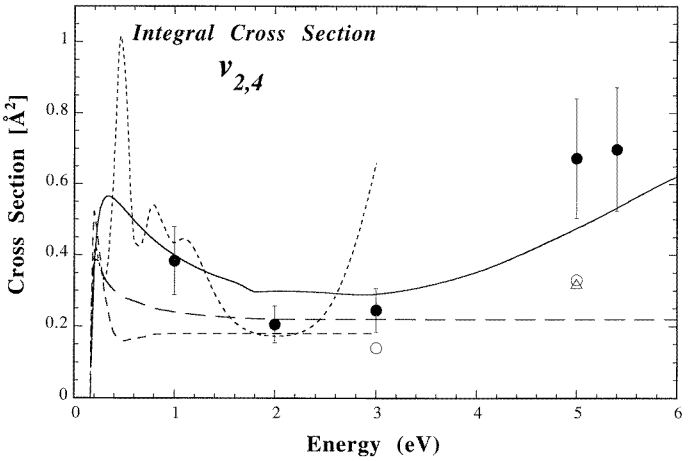

Figure 14. Integral cross section for the excitation of the $\nu_{2,4}$ composite vibrational mode between 0 and 6 eV. ●, present results; ○, Tanaka *et al* (1983); △, Shyn (1991); ——, Althorpe *et al* (1995); — — —, Haddad (1985); – – –, Schmidt (1991); - - -, Hildebrandt (1996).

vibrational excitation of methane (Rohr 1977, 1980, Sohn *et al* 1983, 1986), neither these measurements, nor to our knowledge any other high-resolution differential measurements, indicate structures of the strength or at the energies predicted by the Hildebrandt data. On the other hand the calculations suggest that such peaks are the result of the additional dipole interaction created by the infrared active ν_2 mode.

In figure 15 we compare the present integral vibrational $\nu_{1,3}$ data with the earlier experiments and calculations discussed above for the $\nu_{2,4}$ mode. In addition, we also show the results of a complex Kohn variational calculation by Rescigno. Once again the overall trends that were observed in the data and calculations for the $\nu_{2,4}$ mode are seen here for

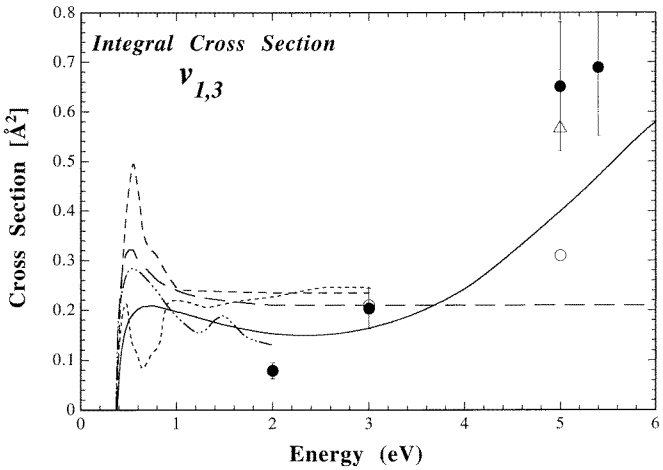

Figure 15. Integral cross section for the excitation of the $\nu_{1,3}$ composite vibrational mode between 0 and 6 eV. ●, present results; *et al* (1995); —···—, Rescigno (1994); — — —, Haddad (1985); – – –, Schmidt (1991); - - -, Hildebrandt (1996).

the $\nu_{1,3}$ mode. In particular, we highlight the reasonable agreement between the present cross section and the calculations of Althorpe *et al* up to fairly high collision energies.

5. Conclusions

The present body of absolute experimental and calculated cross sections for low-energy elastic scattering and vibrational excitation of methane goes some way to resolving a number of outstanding issues regarding the angular and energy dependences and the magnitudes of these cross sections. Very good agreement with the elastic DCS data of Boesten and Tanaka was found at most energies. We note that the elastic DCS of Boesten and Tanaka were also measured using a variation of the relative flow technique used in the present work. In general, there was also good agreement between the present experimental and theoretical elastic DCS, indicating that the SCE theory is providing an accurate description of the scattering process in the energy range between 0.5 and 6 eV. We note that this level of agreement between theory and experiment is quite unusual for the field of electron–polyatomic molecule scattering.

The good agreement between the present measurements and those of Boesten and Tanaka at the elastic DCS level is also reflected in the integral elastic cross sections. In addition, the present elastic data are also in fair agreement with the elastic ICS of Sohn *et al* and the calculation of Althorpe *et al*, particularly at energies above a few eV. Similar observations can also be made with respect to the present study and earlier data, both for beam and swarm measurements, for the elastic momentum transfer cross section. In this case, however, the present results suggest that the swarm cross section of Haddad is superior to that of Hildebrandt with regard to the depth of the R–T minimum. This result is a little surprising as the Hildebrandt measurement should, in principle, be a more exact one.

Grand total cross sections were derived from the present measurements and crossed checked, for self-consistency, against the previous, very accurate attenuation data. The present grand total cross sections were found to be in excellent agreement with the

attenuation results over the entire energy range (0.6–5.4 eV) considered.

For vibrational excitation of the $\nu_{2,4}$ and $\nu_{1,3}$ composite modes the situation is not so clear cut. On the one hand, whilst the present $\nu_{1,3}$ DCS were often in fair agreement with at least one of the earlier measurements, the current $\nu_{2,4}$ DCS were, at each energy, typically much larger in magnitude over the entire angular range than the earlier attempts. This observation is consistent with the previous measurements of Rohr (1977, 1980), Tanaka *et al* (1982, 1983) and Shyn (1991) suffering from the effects of nonlinearities in the response function of their energy analysers. Finally, we note that the present $\nu_{2,4}$ and $\nu_{1,3}$ ICS were found to be in rather good agreement with the earlier theoretical results of Althorpe *et al* (1995). Agreement with the swarm-derived ICS of Hildebrandt, for the $\nu_{2,4}$ channels at 1 and 2 eV, was also good. Whilst we are not in a position to comment definitively on the multiple, near-threshold structure observed by Hildebrandt in both the $\nu_{2,4}$ and $\nu_{1,3}$ ICS, we are not convinced that it has a physical basis. It is not consistent with high-resolution near-threshold beam experiments or with the manifestation of the single dipole-induced peak found in the calculation of Althorpe *et al* (1995). Indeed, when one notes that both the integral elastic cross section and the integral vibrational excitation cross sections have similar magnitudes in the R–T minimum region, it is possible that to some extent the large complex structure reported in the swarm-derived vibrational cross section is compensated in the swarm analysis by the deep, narrow elastic momentum transfer cross section.

Acknowledgments

It is a pleasure to acknowledge the skills of the technical staff of the Electron Physics Group in keeping the apparatus up and running. CTB gratefully acknowledges a Scholarship from the Freiderich Ebert Foundation (Germany), JCG the ANU Graduate School for the provision of a Scholarship and MJB and SJB the ANU Institute of Advanced Studies and The Flinders University of South Australia for the provision of a collaborative research grant. The computational results were supported by a grant from the EU (contract no ERBCHRXCT920013) from the Human Capital and Mobility Programme.

References

Althorpe S C, Gianturco F A and Sanna N 1995 *J. Phys. B: At. Mol. Opt. Phys.* **28** 4165
Barbarito E, Basta M, Calicchio M and Tessari G 1979 *J. Chem. Phys.* **71** 54
Bloor J E and Sherrod R E 1986 *J. Phys. Chem.* **90** 5508
Boesten L and Tanaka H 1991 *J. Phys. B: At. Mol. Opt. Phys.* **24** 821
Brunger M J, Buckman S J and Newman D S 1990 *Aust. J. Phys.* **43** 665
Brunger M J, Buckman S J, Newman D S and Alle D T 1991 *J. Phys. B: At. Mol. Opt. Phys.* **24** 1435
Curry P J, Newell W R and Smith A C H 1985 *J. Phys. B: At. Mol. Phys.* **18** 2303
Dababneh M S, Hsieh Y-F, Kauppila W E, Kwan C K, Smith S J, Stein T S and Uddin M N 1988 *Phys. Rev.* A **38** 1207
Ferch J, Granitza B and Raith W 1985 *J. Phys. B: At. Mol. Phys.* **18** L445
Floeder K, Fromme D, Raith W, Schwab A and Sinapius G 1985 *J. Phys. B: At. Mol. Phys.* **18** 3347
Gianturco F A, Jain A and Rodriguez-Ruiz J A 1993 *Phys. Rev.* A **48** 4321
Gianturco F A, Lucchese R R, Sanna N and Talamo A 1994 *Electron Scattering from Molecules, Surfaces and Clusters* ed H Ehrhardt and L A Morgan (New York: Plenum) p 1236
Gianturco F A, Rodriguez-Ruiz J A and Sanna N 1995a *J. Phys. B: At. Mol. Opt. Phys.* **28** 1287
——1995b *Phys. Rev.* A **52** 1257
Gulley R J, Alle D T, Brennan M J, Brunger M J and Buckman S J 1994 *J. Phys. B: At. Mol. Opt. Phys.* **27** 2593
Haddad G 1985 *Aust. J. Phys.* **38** 672
Hildebrandt M 1996 Private communication
Jain A 1986a *Phys. Rev.* A **34** 954

——1986b *Phys. Rev.* A **34** 3707
Jain A and Thompson D G 1982 *J. Phys. B: At. Mol. Phys.* **15** L631
Jones R K 1985 *J. Chem. Phys.* **82** 5424
Kanik I, Trajmar S and Nickel J C 1992 *Chem. Phys. Lett.* **193** 281
Khakoo M A and Trajmar S 1986 *Phys. Rev.* A **34** 138
Lengsfield B H, Rescigno T N and McCurdy C W 1991 *Phys. Rev.* A **44** 4296
Lohmann B and Buckman S J 1986 *J. Phys. B: At. Mol. Phys.* **19** 2565
Lunt S L, Randell J, Ziesel J P, Mrotzek G and Field D 1994 *J. Phys. B: At. Mol. Opt. Phys.* **27** 1407
Mapstone B and Newell W R 1992 *J. Phys. B: At. Mol. Opt. Phys.* **25** 491
McNaughten P, Thompson D G and Jain A 1990 *J. Phys. B: At. Mol. Opt. Phys.* **23** 2405
Müller R, Jung K, Kochem K-H, Sohn W and Ehrhardt H 1985 *J. Phys. B: At. Mol. Phys.* **18** 3971
Nesbet R K 1979 *Phys. Rev.* A **20** 58
Nickel J C, Zetner P W, Shen G and Trajmar S 1989 *J. Phys. E: Sci. Instrum.* **22** 730
Nishimura H and Sakae T 1990 *Japan. J. Appl. Phys.* **29** 1372
Rescigno T N 1994 *Electron Scattering from Molecules, Surfaces and Clusters* ed H Ehrhardt and L A Morgan (New York: Plenum) p 1
Rohr K 1977 *J. Phys. B: At. Mol. Phys.* **10** 2215
——1980 *J. Phys. B: At. Mol. Phys.* **13** 4897
Schmidt B 1991 *J. Phys. B: At. Mol. Opt. Phys.* **24** 4809
Shyn T W 1991 *J. Phys. B: At. Mol. Opt. Phys.* **24** 5169
Shyn T W and Cravens T E 1990 *J. Phys. B: At. Mol. Opt. Phys.* **23** 293
Sohn W, Jung K and Ehrhardt H 1983 *J. Phys. B: At. Mol. Phys.* **16** 891
Sohn W, Kochem K-H, Scheuerlein K M, Jung K and Ehrhardt H 1986 *J. Phys. B: At. Mol. Phys.* **19** 3625
Sueoka O and Mori S 1986 *J. Phys. B: At. Mol. Phys.* **19** 4035
Tanaka H, Kubo M, Onodera N and Suzuki A 1983 *J. Phys. B: At. Mol. Phys.* **16** 2861
Tanaka H, Okada T, Boesten L, Suzuki T, Yamamoto T and Kubo M 1982 *J. Phys. B: At. Mol. Phys.* **15** 3305
Yuan J 1988 *J. Phys. B: At. Mol. Opt. Phys.* **21** 2737
Zecca A, Karwasz G, Brusa R S and Szmytkowski C 1991 *J. Phys. B: At. Mol. Opt. Phys.* **24** 2747